Tracking and Optimal Control Problems in Human Head/Eye Coordination

Indika Wijayasinghe[1], Eugenio Aulisa[1], Bijoy K. Ghosh[1], Stefan Glasauer[2,3] and Olympia Kremmyda[4]

***Abstract*— Human head and eye rotate in coordination to rapidly project images of targets from the visual space. Once a target is fixated, the head/eye complex maintains the stability of the image, even while the head continues to move. The dynamics of the head is constrained by Donders' Law whereas the final position of the eye satisfies Listing's constraint with respect to the final position of the head. The vestibuloocular reflex rotates the eye opposite to the forward movement of the head in order to compensate and maintain image stability. Using a dynamic model of the head and eye, the eye movement is modeled as a tracking control problem, where the tracking signal depends on the head movement trajectory. The torques required for the head and eye movements are computed by minimizing a suitable cost function. The paper computes the optimal torque and compares simulation results with experimentally measured data on human head/eye movement.**

***Index Terms*— Head Movement, Eye Movement, Listing's Law, Donders' Surface, Vestibulo-ocular reflex, Optimal Control, Tracking.**

I. Introduction

Neurologists, physiologists and engineers have been interested in modeling and control of the eye since 1845 with notable studies conducted by Listing [1], Donders [2] and Helmholtz [3]. Specifically, it has been observed that, when the head coordinates are fixed, the oculomotor system chooses just one angle of ocular torsion for any one gaze direction (see Donders [2]). In fact, the axes of rotations of the eye, away from the primary gaze direction, always lie on a fixed plane called the Listing's plane. Since its discovery, the so called Donders' law, has also been applied to the head (see Ceylan et al. [4]), which is mechanically able to rotate torsionally, but which normally adopts just one torsional angle for any one facing direction, see Straumann et. al. [5], Glenn and Vilis [6], Tweed and Vilis [7]. A geometric consequence of the Donders' Law is that the three dimensional vectors that represent the axes of rotations[1] of the head are not spread out in a 3-D volume but instead fall in a single two-dimensional surface known as the Donders' surface. When the head and eye are both allowed to move freely, the situation is a bit more complicated (see [8]). In an attempt to capture a target, the eye violates the Listing's constraint and locks on to the target. In so doing the eye saccades and may move on to an eccentric position, ahead of the head. The eye does not stay in that position but rotates backwards, while the head moves forward, satisfying Donders' constraint, towards the target. As the eye recovers from its initial surge, the vestibulo-ocular reflex guarantees that the image on the retina remains invariant. In other words, the head movements are precisely compensated by the backward movement of the eye. Additionally it has been observed that, in the steady state, when both the head and the eye have momentarily reached a point of immobility, the ocular torsion is once again close to zero. It indicates that at the point of immobility Listing's constraint is satisfied.

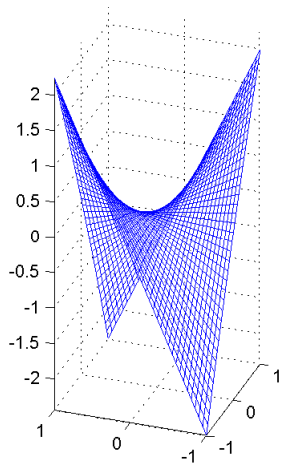

Fig. 1: Donders' surface (7) after scaling m_0 to 1, has been sketched. The scaled coordinates are $\bar{m}_i = \frac{m_i}{m_0}$ for $i = 1,2,3$, where $[m_0, m_1, m_2, m_3]^T$ is the quaternion. The coordinate $\bar{m}_3$ along the vertical line shows the nonzero torsion.

During the process of acquiring a target, the head closely follows the eye and settles on points that satisfy the Donders' constraint on the head movement and meets the Listing's constraint that the eye satisfies at points of immobility when both head and the eye are stationary. It would appear that, the eye hops unrestricted to acquire a target and the head follows the eye, eventually meeting the Donders' and the Listing's constraints. In reality, however, the eye moves backwards even after acquiring a target to compensate for the forward movement of the head.

The paper is based upon work supported in part by the National Science Foundation under Grant No. 1029178. Any opinions, findings, and conclusions or recommendations expressed in this material are those of the author(s) and do not necessarily reflect the views of the National Science Foundation. Part of this research is also supported by BMBF Grant No. 01*E*00901.

[1]Dept. of Mathematics and Statistics, Texas Tech University, Lubbock, TX, USA bijoy.ghosh@ttu.edu

[2]Integrated Research and Treatment Center for Vertigo IFB-LMU, University Clinic Munich, Munich, Germany

[3]Center of Sensorimotor Research, Ludwig-Maximilians University, Munich, Germany

[4]Dept. of Neurology, Ludwig-Maximilians University, Munich, Germany

[1]See later part of the paper for a precise definition of the axis of rotation.

We choose a head trajectory, a stationary point target and derive eye trajectory that captures the target followed by a backward eye movement that compensates for the head motion. The head movement trajectory assumes that the Donders' constraint is satisfied for all points on the trajectory. Likewise, the eye movement trajectory is computed assuming that Listing's constraint is satisfied when both eye and the head have reached their terminal points. This trajectory is computed, ensuring that the orientation of the eye remains invariant with respect to a fixed global coordinate system[2].

It is easy to see that the problem of acquiring a target fixed in space with respect to a global coordinate system, is equivalent to the problem of trajectory tracking that the eye control system has to satisfy with respect to the coordinate system attached to the head. Subsequent to target acquisition, the tracking controls are generated by vestibulo-ocular reflex (VOR), which ensures that the eye is rotated backwards to compensate for the head movement. The effect of VOR on the eye is modeled as an open loop tracking controller (see [9]). We illustrate our results by plotting the eye trajectories. In all, three trajectories have been plotted in this paper. The first trajectory is the head movement with respect to a fixed coordinate system attached to the torso. The second trajectory is the eye movement with respect to the same coordinate system attached to the torso. The eye moves to fixate on a target and subsequently its orientation does not change (being compensated by VOR), even though the head continues to move. The third trajectory is the eye movement with respect to a moving coordinate system attached to the head. In this trajectory, the eye moves forward to acquire the target and then moves backward to compensate for the forward motion of the head. Effect of VOR is displayed as a backward movement of the eye, in this third trajectory.

Ideally, the eye movement control system anticipates the head trajectory in order to compute the trajectory it needs to track. In this paper, we assume that the head trajectory is entirely known and the eye movement is simulated as an optimal tracking problem. Two alternative schemes have been introduced in this paper to compute the head trajectory. In the first scheme, we compute the trajectory by solving a tracking problem where the tracking signals are obtained by interpolating observed head movement data of a human subject. In the second scheme, we compute the trajectory by constraining the initial and final orientation of the head, obtained once again from observed data. In both the schemes, the computed trajectories optimize a cost function that we introduce later in this paper[3]. The simulated Head and Eye movement trajectories are compared with experimentally measured data on human head/eye movement.

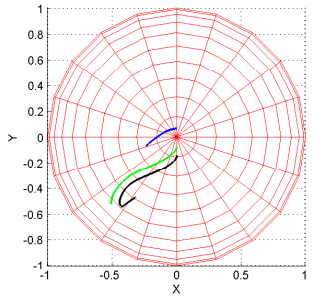

(a) Actual trajectories using measured data from one human subject.

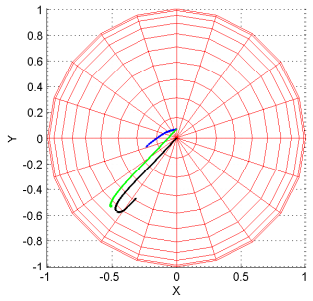

(b) Simulated trajectories from dynamic models while head is tracking

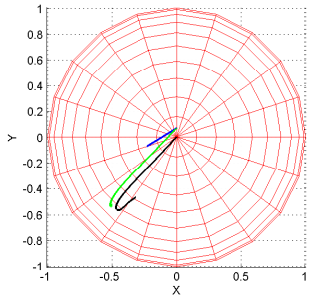

(c) Simulated trajectories from dynamic models while head moves optimally satisfying boundary constraints.

Fig. 2: The short (blue) trajectory on top is the head movement. The green trajectory in the middle is the eye movement with respect to a fixed global coordinate. The bottom (black) trajectory corresponds to the eye movement with respect to the moving head coordinates. All trajectories are plotted after projecting them onto the gaze (heading) space $\mathbf{S}^2$.

II. Listing's and Donders' Constraints

We assume a global coordinate system fixed with respect to the torso and that the head and eye orientations are measured with respect to this coordinate system and that every orientation is a point in **SO(3)**. Without any loss of generality, the head is assumed to be initially located at the identity matrix **I**. Following [10], [11], we describe a coordinate system on **SO(3)** using a coordinate map on $\mathbf{S}^3$ as follows:

$$\rho \; : \; [0,2\pi] \times [0,\pi] \times \left[-\frac{\pi}{2},\frac{\pi}{2}\right] \rightarrow \mathbf{S}^3 \qquad (1)$$

[2] A coordinate system attached to the torso.

[3] We do not claim that the human brain actually uses the proposed cost function. We do claim that for the two schemes, introduced on head movement, the simulated eye and head trajectories closely mimic observed data.

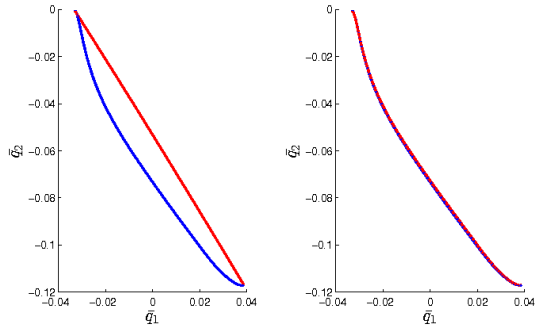

(a) Optimal trajectory (red) in comparison to the actual trajectory (blue)

(b) Simulated tracking trajectory (red) in comparison to the actual trajectory (blue)

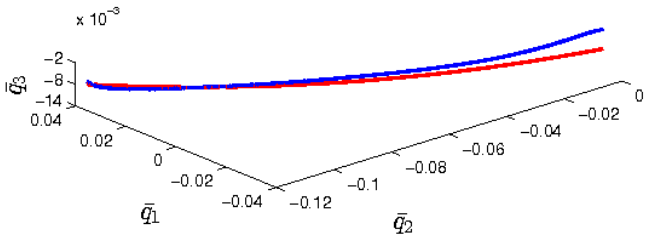

(c) Optimal trajectory (red) in comparison to the actual trajectory (blue)

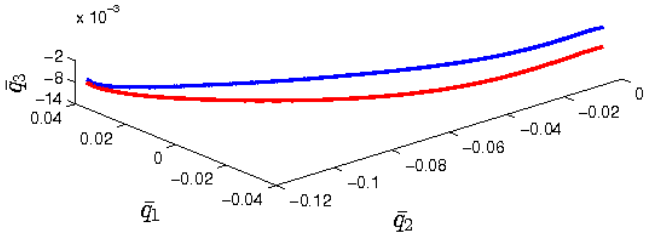

(d) Simulated tracking trajectory (red) in comparison to the actual trajectory (blue)

Fig. 3: Actual and simulated head trajectories using scaled coordinates $\bar{q}_i = \frac{q_i}{q_0}$ for $i = 1,2,3$, where $[q_0,q_1,q_2,q_3]^T$ is the unit quaternion. The trajectories in Fig. 3d differ because the actual trajectory (blue) does not satisfy Donders' constraint precisely whereas the simulated trajectory (red) does. This difference is not visible on the projected plane in Fig. 3b. In Fig. 3a, the optimal trajectory (red) is almost a straight line whereas the actual trajectory (blue) is not.

where

$$\rho(\theta,\phi,\alpha) = \begin{pmatrix} \cos\frac{\phi}{2} \\ \sin\frac{\phi}{2}\cos\theta\cos\alpha \\ \sin\frac{\phi}{2}\sin\theta\cos\alpha \\ \sin\frac{\phi}{2}\sin\alpha \end{pmatrix}. \tag{2}$$

Next we consider the map **rot** from [11], between $\mathbf{S}^3$ and **SO(3)** given by

$$\text{rot} : \mathbf{S}^3 \to \mathbf{SO(3)}. \tag{3}$$

The image of the composite map "rot $\circ\, \rho(\theta,\phi,\alpha)$" is a rotation matrix which rotates a vector in $\mathbf{R}^3$ around the axis

$$\tan\frac{\phi}{2}\ (\cos\theta\cos\alpha,\ \sin\theta\cos\alpha,\ \sin\alpha)^T \tag{4}$$

by a counterclockwise angle ϕ. Every point in $\mathbf{S}^3$ is considered as a unit quaternion [12]. The map **rot** is a $2-1$ map and every quaternion q and $-q$ are mapped to the same rotation matrix in **SO(3)**. The angle parameter vector (θ,ϕ,α) can therefore be viewed as a coordinate on **SO(3)**. The vector (4) is called the *'axis of rotation'*.

Donders' law states that for head rotation, the axes of rotations lie in a surface that goes by the name **Donders' Surface** [10]. In order to describe this surface, the **torsion** angle parameter α is often written as a function of the other two parameters θ and ϕ. When the torsion is zero, i.e. when $\alpha = 0$, the Donders' surface becomes a plane that goes by the name **Listing's Plane** [11]. When the head is restricted to be fixed, orientations of the eye of an individual lie on the Listing's plane. When head is free to move, which is the case described in this paper, eye orientations are not always constrained by the Listing's plane. However when the eye has fixated on a target and when both eye and head reaches a point of immobility, Listing's constraint is once again satisfied.

When a target is introduced in the visual space, eye rotates to fixate on the target as quickly as possible. We assume that this motion takes place in $\mathbf{S}^3$. Let $e = [e_0,e_1,e_2,e_3]^T$ be the coordinates (quaternion coordinates) of the target with respect to a fixed global coordinate system (assumed attached to the torso in this paper). Furthermore, we assume that $m(t) = [m_0(t),m_1(t),m_2(t),m_3(t)]^T$ are the quaternion coordinates of the moving head, with respect to the same global coordinate system. Finally, we assume that at $t = 1$, the head comes to a stop and the eye is fixated on the target. At this time, the eye satisfies Listing's constraint with respect to the head. The following Lemma describes the constraint between $m(1)$ and e dictated by the Listing's constraint:

Lemma I: A necessary and sufficient condition for the eye to satisfy Listing's constraint with respect to the head is

$$e_0m_3(1) + e_2m_1(1) = e_1m_2(1) + e_3m_0(1). \tag{5}$$

Proof of lemma I: The quaternion coordinates of the eye with respect to the moving head coordinates is given by

$$[m_0(t),-m_1(t),-m_2(t),-m_3(t)] \bullet [e_0,e_1,e_2,e_3] \tag{6}$$

where $\bullet$ denotes quaternion multiplication (see [13] for a definition). For the eye to satisfy Listing's constraint with respect to the head, the last coordinate of the product in (6) must be zero at $t = 1$. The condition (5) easily follows. □

Of course, at all time 't', the head coordinates satisfy an additional constraint imposed by Donders' law. In this paper we assume that the Donders' surface is quadratic and is of the form

$$m_3m_0 = h_0m_0^2 + 2h_1m_1m_0 + 2h_2m_2m_0 + h_{11}m_1^2 + h_{22}m_2^2 + 2h_{12}m_1m_2, \tag{7}$$

where the parameters h_* are assumed known.

Remark I: We would assume that as soon as the presence of a target is detected, the final head orientation is anticipated. The coordinates $e = [e_0,e_1,e_2,e_3]$ satisfying the target gaze direction and the Listing's constraint (5) are easily computed. If the head follows a trajectory $m(t)$, the eye has

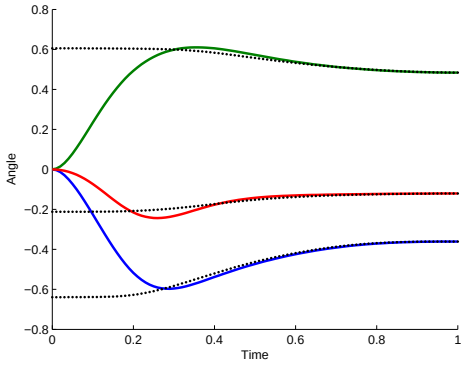

(a) Eye parameters tracking while the head tracks measured trajectory of a human subject

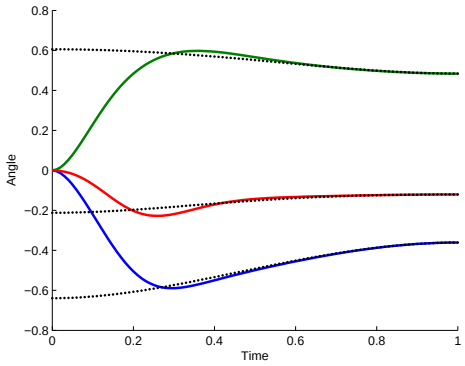

(b) Eye parameters tracking while the head moves optimally between initial and final point of a measured trajectory from a human subject.

Fig. 4: Top (Green), Middle (Red) and the Bottom (Blue) curves are the angles ϕ_2, ϕ_3 and ϕ_1 respectively from the Tait-Bryan parametrization [14].

to follow the trajectory $\xi(t) = m(t)^{-1} \bullet e$ in order to maintain 'orientation stability' of image. It would imply that the eye controller has to track the signal $\xi(t)$.

Remark II: Head movement data was recorded in conjunction with eye movement and for complete details we would refer to Glasauer et. al. [15] and Kremmyda et. al. [16]. Data was recorded from 7 subjects, aged 25 to 38 years with no known neurological or orthopedic disorders. For $3D$ eye movement recordings, a dual search coil was used on the left eye (Skalar, Delft, The Netherlands) and for the 3D head movements, two coils mounted on a head ring at 90 degrees angle between them was used. Both head and eye coil measured absolute position in space. Therefore, when the head was allowed to move, the eye coil recorded gaze (combined eye and head) movements. The subjects were seated in complete darkness inside a magnetic field and were instructed to follow a laser dot. Subjects had to follow the target with a combination of natural eye and head movements. The laser dot jumped randomly between the center and eight peripheral positions, so that each final position is reached from a different initial position. Head and Eye movement data from one subject, whose Donders' surface is sketched in Fig. 1, is analyzed further in this paper.

TABLE I: For multiple tracking manoeuvres, the final head and the eye positions are compared with the closest points on the Donders' surface and Listing's plane respectively. The table displays the absolute errors in radians computed as angle between vectors on $\mathbf{S}^3$. The root mean square of the Donders' error is 0.0098 and the Listing's error is 0.0451 in radians

Direction	Donders' Error	Listing's Error
1	0.0147	0.0036
1	0.0035	0.0380
1	0.0046	0.0263
1	0.0020	0.0075
1	0.0088	0.0569
1	0.0221	0.0612
2	0.0021	0.0852
2	0.0027	0.0821
2	0.0096	0.0753
2	0.0049	0.0858
3	0.0092	0.0236
3	0.0048	0.0363
3	0.0084	0.0462
3	0.0023	0.0656
3	0.0014	0.0602
3	0.0127	0.0836
3	0.0123	0.0769
3	0.0082	0.0422
4	0.0010	0.0465
4	0.0056	0.0334
4	0.0008	0.0120
4	0.0059	0.0483
5	0.0012	0.0018
5	0.0016	0.0517
5	0.0018	0.0166
5	0.0048	0.0300
5	0.0055	0.0366
6	0.0134	0.0292
6	0.0034	0.0029
6	0.0014	0.0237
6	0.0228	0.0288
7	0.0096	0.0290
7	0.0055	0.0162
7	0.0015	0.0237
7	0.0164	0.0101
8	0.0005	0.0010
8	0.0275	0.0077
8	0.0125	0.0391
8	0.0089	0.0057

While this subject performs multiple tracking manoeuvres along 8 different directions, we display in Table I the extent to which Listing's and Donders' laws are satisfied when the subject has acquired the target and the eye and the head have come to rest. Similar calculations have been repeated for other six subjects as well. The point of this remark is that the Donders' and Listing's constraints are closely supported by observed data.

III. Head/Eye Movement Dynamics

The head and eye movement trajectories are simulated using an appropriate Lagrangian formulation, the main ideas of which are already sketched in [10], [11]. We rewrite the main steps using coordinates (θ, ϕ, α) from section II.

Let $q(\theta, \phi, \alpha)$ be a parametrization of the manifold $\mathbf{S}^3$.

We define Riemannian metric on $\mathbf{S}^3$ given by

$$G = \begin{pmatrix} q_\theta \cdot q_\theta & q_\theta \cdot q_\phi & q_\theta \cdot q_\alpha \\ q_\phi \cdot q_\theta & q_\phi \cdot q_\phi & q_\phi \cdot q_\alpha \\ q_\alpha \cdot q_\theta & q_\alpha \cdot q_\phi & q_\alpha \cdot q_\alpha \end{pmatrix}, \tag{8}$$

where $q_\gamma = \frac{\partial q}{\partial \gamma}$ and 'dot' in (8) is the vector dot product. Let us define $X = (\theta, \phi, \alpha)^T$ to be the vector of angle variables. As in [11], we would define the Kinetic Energy[4] KE as

$$KE = \frac{1}{2} \dot{X}^T G \dot{X}. \tag{9}$$

If the potential energy is represented by V, the Lagrangian of the head movement system can be written as

$$L = KE - V. \tag{10}$$

The equation of motion on the Donders' surface, using the Euler Lagrange equation can now be described as

$$\frac{d}{dt}\frac{\partial L}{\partial \dot{\gamma}} - \frac{\partial L}{\partial \gamma} = \tau_\gamma \tag{11}$$

where γ can be the angle variable θ, ϕ or α and where τ_γ is the generalized torque input (to be viewed as the control input) to the system. The resulting equations of motion can be expressed as

$$G\ddot{X} + \dot{G}\dot{X} - \frac{1}{2}\dot{X}^T \nabla_X G \dot{X} + \nabla_X V = \Gamma \tag{12}$$

where $\Gamma = (\tau_\theta \quad \tau_\phi \quad \tau_\alpha)^T$ and where ∇_X is the gradient operator with respect to X defined as

$$\nabla_X = \left(\frac{\partial}{\partial \theta}, \frac{\partial}{\partial \phi}, \frac{\partial}{\partial \alpha} \right). \tag{13}$$

Remark III: In this paper, the potential energy term V is assumed to be identically zero. It would follow that the head and the eye are not potentially driven but instead, as we see in the next section, driven by an optimal control.

IV. Tracking and Optimal Rotation of Human Head and Eye

When a target is visible, the head controller decides on rotating the head towards the target. In this paper we assume that the final orientation of the head is known, both to the head and the eye controller. We use different strategy to compute the actual path the head takes to reach the final orientation.

A. Head Tracking an observed head movement while eye acquires a target

We consider a cost function given by

$$J = \int_0^1 \frac{\alpha}{2}\Gamma^T\Gamma + \frac{\beta}{2}C^T C + p^T\left(F - \ddot{X}\right) + \lambda^T D + \frac{1}{2}\dot{\lambda}^T \varepsilon \dot{\lambda}\, dt \tag{14}$$

[4]The head is assumed to be a perfect sphere with mass distributed uniformly. The rotation is assumed to be about the center of the sphere. In this case, the usual definition of KE = $\omega^T I\, \omega$, documented in Physics (see [17]), differs from the definition (9) by a constant scale factor, where ω is the angular velocity vector and I is the diagonal moment of inertia matrix. The parameter I for eye and head are chosen to be different.

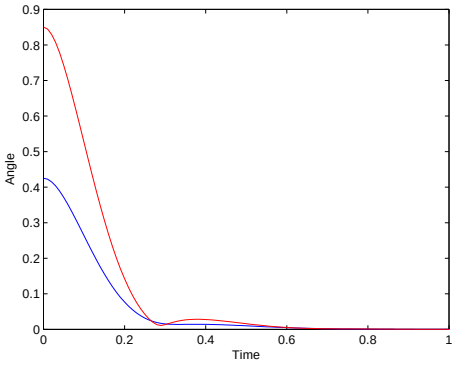

(a) Head is following optimal trajectory with constrained initial and final points.

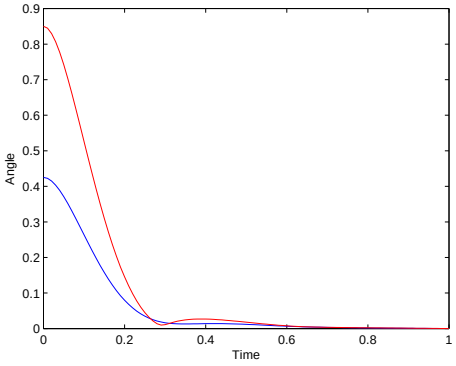

(b) Head is tracking observed trajectory from a human subject.

Fig. 5: Blue: Angle between the eye quaternion and the target represented as a quaternion. Red: Angle between the eye direction and the target direction.

where $\ddot{X} = F$ is the equations of motion (12), $D \equiv 0$ is the Donders' constraint (7), $C = (A(t) - X)$ and $A(t)$ is the trajectory to track. In this case $A(t)$ is the measured head trajectory data projected on to **DOND**[5]. The parameters α and β are constants to be chosen for each simulation. We have chosen $\alpha = 2$ and $\beta = 2,000,000$ to obtain a near perfect tracking of the head trajectory. The initial and the final orientations of the head are chosen to match measured trajectory of the head projected on to **DOND**. Boundary conditions are prescribed by choosing $(X(0), \dot{X}(0), X(1), \dot{X}(1))$.

The Hamiltonian [11] for this problem is defined as

$$H = \frac{\alpha}{2}\Gamma^T\Gamma + \frac{\beta}{2}C^T C + p^T F + \lambda^T D. \tag{15}$$

Using this notation, we write

$$J = \int_0^1 \left[H - p^T \ddot{X} + \frac{1}{2}\dot{\lambda}^T \varepsilon \dot{\lambda} \right] dt. \tag{16}$$

Applying the principle of variation, we obtain the following

[5]Using Tait Bryan Parametrization [14], the projection was achieved by adjusting ϕ_3 while keeping ϕ_1 and ϕ_2 unchanged. This amounted to rotating the head keeping the 'heading' direction fixed.

set of Hamilton's equations.

$$\begin{aligned} \dot{X} &= \frac{\partial H}{\partial p} = F;\ \dot{p} = \frac{\partial H}{\partial X} - \frac{d}{dt}\left(\frac{\partial H}{\partial \dot{X}}\right) \\ \dot{\lambda} &= \varepsilon^{-1}\frac{\partial H}{\partial \lambda};\ \Gamma = -\frac{1}{\alpha}G^{-1}p, \end{aligned} \tag{17}$$

where the optimal control Γ is obtained by setting $\frac{\partial H}{\partial \Gamma} = 0$.

B. Head moving along an optimal trajectory while eye acquires a target

In this case, the head is not required to follow a measured trajectory but is constrained by an initial and final value of the state. The cost function, we consider is given by (14) where we assume that the term that involves β is absent, i.e. choose $\beta = 0$. Likewise, the Hamiltonian is given by (15), where we assume $\beta = 0$. Using variational principle, we write down equations given by (17) including the optimal control Γ obtained as before. The parameter α is chosen as 2.

C. Eye moving along a trajectory

In order to compensate for the head movement, the eye has to follow the trajectory already described in Remark I. In order to compute the tracking controller, we would consider (17), where the term $A(t)$ has to be adjusted in defining the Hamiltonian H in (15). The parameters are chosen as $\alpha = 2$ and $\beta = 1,000$. Since the intermediate points of the eye trajectory does not satisfy a constraint in **SO(3)**[6], the term $\lambda^T D$ in (14) is absent. It would follow that the Hamilton's equation would be given by

$$\begin{aligned} \dot{X} &= \frac{\partial H}{\partial p} = F;\ \dot{p} = \frac{\partial H}{\partial X} - \frac{d}{dt}\left(\frac{\partial H}{\partial \dot{X}}\right) \\ \Gamma &= -\frac{1}{\alpha}G^{-1}p, \end{aligned} \tag{18}$$

where Γ is the optimal control.

V. Results and Discussions

Rotational Dynamics of the head and the eye are both described by an equation of the form (12), already introduced in [14]. In this paper, we assume that the potential energy term V is absent and that the eye and head differ in their respective moment of inertias, by a scale factor. Head movements are assumed to satisfy Donders' constraint (7), throughout its trajectory. All results in this section are stated with respect to one specific healthy human subject. The associated Donders' surface for this subject, shown in Fig. 1, has already been derived in [14].

Head movement trajectories are displayed in Fig. 3 in three ways. The orientation of the head is represented using a unit quaternion (as described in (3)). The unit quaternion, represented as $[q_0, q_1, q_2, q_3]^T$, has coordinates described by $\bar{q}_i = \frac{q_i}{q_0}$, for $i = 1, 2, 3$. In Figs. 3c, 3d, head trajectories are plotted using the three scaled coordinates. Since the head orientations, satisfy Donders' constraint (7)[7] at all times, one can eliminate one of the three coordinates and plot the head trajectories on a plane using coordinates $(\bar{q}_1, \bar{q}_2)$. This has been displayed in Figs. 3a, 3b.

We now describe the three ways, head trajectories have been displayed in Fig. 3. The blue trajectories are the actual trajectories measured from the human subject. The red trajectories, on the other hand are simulated trajectories. The simulation is carried out two ways. In the first method, we have considered a cost function (14) that puts a heavy weight on the tracking error. The goal is to track the actual trajectory as closely as possible. In Fig. 3b, we see that the tracking error is virtually absent, whereas the three dimensional plot in Fig. 3d shows that the tracking error is introduced because the actual trajectory does not precisely satisfy the Donders' constraint. In the second method, we have considered the same cost function (14), while we set the parameter $\beta = 0$. The goal is to construct an optimal trajectory that joins the initial and the final points on the state space. Simulation results are displayed in Figs. 3a and 3c. Note that, for each of the two cases, the head trajectories are simulated by solving the Hamilton's equation (17) assuming a suitable boundary condition on the state variable.

We now move on to the problem of simulating the eye movement trajectories. Note that the eye movements are simulated as a tracking problem, where the final orientation of the eye is computable from the final orientation of the head[8] and the fact that the final eye orientation satisfies Listing's constraint (5) with respect to the final head orientation. The final orientation of the eye is used to compute a tracking signal $\xi(t)$ (described in Remark I), for the eye to track. Note that when the eye track $\xi(t)$ perfectly, the head eye pair remains fixated on the stationary target, with a specific orientation that does not change in time. Hence image of the target is invariant on the retina.

Once the tracking signal $\xi(t)$ is computed, the tracking strategy is similar to the head tracking problem, except that the eye is not constrained on **SO(3)**. We obtain Hamilton's equation of the form (18), which we solve subject to a suitable boundary condition. The results are displayed in Fig. 4, where the dotted trajectory is the tracking signal $\xi(t)$. In the subfigure 4a, the tracking signal $\xi(t)$ is computed by assuming that the head tracks the measured head trajectory of the human subject. In the subfigure 4b, the head follows the optimal trajectory subject to the boundary conditions. In Fig. 4, we did not use the scaled coordinates of the unit quaternion (see Fig. 3). Instead, a new Tait Bryan coordinates (see [14]) has been used. The two plots in Figs. 4a and 4b are similar, indicating that the actual head movement strategy is perhaps less important for the eye to acquire and stabilize a target on its retina.

The head and the eye movement trajectories are plotted on the gaze space (heading direction for the head) in Fig. 2. The figure has been separated between three subcases considered in this paper. They are the actual and the simulated trajectories of the Head/Eye, assuming that the head either tracks

[6] When the head is free, the eye orientations are not restricted by Listing's constraint

[7] Note that in (7), Donders' surface is described using unit quaternion $[m_0, m_1, m_2, m_3]^T$.

[8] We assume that this information is available to the eye controller as soon as the target is visible.

a given signal or moves optimally satisfying a boundary condition. In each of the three subfigures in Figs. 2a, 2b and 2c, the eye movement trajectories are displayed with respect to the moving head coordinate system and the fixed global coordinate attached to the torso. The point of the two eye movement plots is to show that, in the head coordinate, the eye moves rapidly forward to acquire a target and then it has to move backward to compensate for the forward movement of the head. On the other hand, with respect to the fixed coordinate, eye orientation does not change appreciably once a target is acquired.

To display how good the eye is able to stabilize the image for the two simulated eye trajectories, we compute the angular error between the 'eye orientation', (represented as a unit quaternion vector) and the target orientation (represented as a unit quaternion using the final orientation of the eye). This error plot is displayed in Fig. 5 using 'blue'. We also compute the angular error between the 'eye gaze direction' and the 'target direction' and display the error plot in Fig. 5 using 'red'. The plots show that from the point of view of 'orientation' and 'gaze direction', the image is stabilized as soon as it is captured and this conclusion does not change if the head movement strategy is altered (evident from comparing the plots in Figs. 5a and 5b).

VI. Conclusion

Using dynamical systems and optimal control, in this paper we study the extent to which an eye controller is able to stabilize a target in spite of a possible head movement. Control systems for the eye and the head are derived using Lagrangian mechanics for a rigid sphere undergoing rotation. The eye and the head are assumed to rotate about their center and in this paper, the two centers are assumed to be the same. Target stabilization is achieved by making the eye follow a tracking signal. In order to compute the eye tracking signal, the final orientation of the head is required to be known and available to the eye controller. It is unclear how this orientation is computed.

For both, eye and head, the tracking control is synthesized by optimizing a cost function that has a 'tracking error term' to be minimized. We also consider a case when the head movements are constrained by boundary values. Although detailed quantitative results are not reported in this paper, we do show that the general qualitative solution to the head/eye coordination problem, from the point of view of acquiring and stabilizing a target, is independent of the strategy as to how the head is being moved.

In this paper, we have considered one subject undergoing one specific target acquisition. Future study will include multiple subjects trying to gaze at multiple targets.

References

[1] J. B. Listing, *Beiträge zur physiologischen Optik.* Göttingen: Göttinger Studien, Vandenhoeck und Ruprecht, 1845.

[2] F. C. Donders, "Beiträge zur lehre von den bewegungen des menschlichen auges," *Holländische Beiträge zu den anatomischen und physiologischen Wissenschaften*, vol. 1, pp. 104–145, 1848. Press, 1996.

[3] H. von Helmholtz, *Handbuch der Physiologischen Optik.*, 3^{rd} ed. Leipzig: Vos., 1866, no. 3, Leopold Voss, Hamburg & Leipzig, 1910.

[4] M. Ceylan, D. Y. P. Henriques, D. B. Tweed, and J. D. Crawford, "Task-dependent costraints in motor control: Pinhole goggles make the head move like an eye," *The Journal of Neuroscience*, vol. 20(7), pp. 2719–2730, April. 2000.

[5] D. Straumann, T. Haslwanter, M. C. Hepp-Reymond, and K. Hepp, "Listing's law for the eye, head, and arm movements and their synergistic control," *Exp. Brain Res.*, vol. 86, pp. 209–215, 1991.

[6] B. Glenn and T. Vilis, "Violations of listing's law after large eye and head gaze shifts," *J. Neurophysiol.*, vol. 68, pp. 309–318, 1992.

[7] D. Tweed and T. Vilis, "Listing's law for gaze directing head movements," in *The Head-Neck Sensory Motor System*, A. Berthoz, W. Graf, and P. P. Vidal, Eds. New York: Oxford, 1992, pp. 387–391.

[8] D. Tweed, T. Haslwanter, and M. Fetter, "Optimizing gaze control in three dimensions," *Science*, vol. 281(28), pp. 1363–1365, Aug. 1998.

[9] F. A. Miles and S. G. Lisberger, "Plasticity in the vestibulo-ocular reflex: A new hypothesis," *Annual Review of Neuroscience*, vol. 4, pp. 273–299, 1981.

[10] B. K. Ghosh and I. Wijayasinghe, "Dynamics of human head and eye rotations under Donders' constraint," *IEEE Trans. on Automat. Contr.*, vol. 57(10), pp. 2478–2489, Oct. 2012.

[11] A. D. Polpitiya, W. P. Dayawansa, C. F. Martin, and B. K. Ghosh, "Geometry and control of human eye movements," *IEEE Trans. in Aut. Contr.*, vol. 52(2), pp. 170–180, Feb. 2007.

[12] S. W. Sheppard, "Quaternion from rotation matrix," *Journal of Guidance and Control*, vol. 1(3), pp. 223–224, May-June, 1978.

[13] S. L. Altmann, *Rotations, Quaternions, and Double Groups*. Oxford University Press (Hardcover), 1986; Dover Publications (Paperback)., 2005.

[14] I. Wijayasinghe, J. Ruths, U. Büttner, B. K. Ghosh, S. Glasauer, O. Kremmyda, and J.-S. Li, "Potential and optimal control of human head movement using Tait-Bryan parametrization," *submitted to Automatica*, 2013.

[15] S. Glasauer, M. Hoshi, U. Kempermann, T. Eggert, and U. Büttner, "Three dimensional eye position and slow phase velocity in humans with downbeat nystagmus," *J. Neurophysiol.*, vol. 89, pp. 338–354, 2003.

[16] O. Kremmyda, S. Glasauer, L. Guerrasio, and U. Büttner, "Effects of unilateral midbrain lesions on gaze (eye and head) movements," *Ann. N. Y. Acad. Sci.*, vol. 1233, pp. 71–77, 2011.

[17] J. D. Cutnell and K. W. Johnson, *Physics, Ninth Edition*. Wiley, Jan 3, 2012.